# Nanoscale

Accepted Manuscript


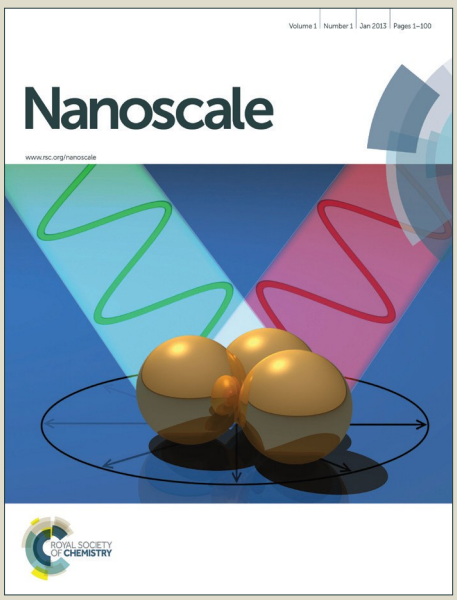





ROYAL SOCIETY OF CHEMISTRY

www.rsc.org/nanoscale

Nanoscale

COMMUNICATION

# Energy transfer in diiodoBODIPY-grafted upconversion nanohybrids

Received 00th January 20xx,
Accepted 00th January 20xx

DOI: 10.1039/x0xx00000x

www.rsc.org/

Laura Francés-Soriano,[a] Marta Liras,[b] Maria Agnieszka Kowalczyk,[c] Artur Bednarkiewicz,[d] Maria González-Béjar,[a,*] Julia Pérez-Prieto[a,*]

**Steady-state and time-resolved emission studies on nanohybrids consisting of $NaYF_4$:Yb,Er and a diiodo-substituted Bodipy (UCNP-IBDP) show that the $Yb^{3+}$ metastable state, formed after absorption of a near-infrared (NIR) photon, can decay via two competitive energy transfer processes: sensitization of IBDP after absorption of a second NIR photon and population of $Er^{3+}$ excited states.**

Understanding resonant energy transfer (RET) processes between emissive nanoparticle donors and organic dye acceptors is of paramount importance for both fundamental photophysics and application oriented studies. Detailed studies on the RET phenomenon can be found in literature mostly regarding Quantum Dots (QDs) donors.[1] By contrast, only few examples of time-resolved studies have been reported for upconversion nanoparticles (UCNPs) acting as RET donors.[2-5]

Whereas QDs undergo down-conversion after excitation, the UCNPs emit in the visible spectral range upon near infrared (NIR) excitation due to multiple intra-configurational $4f^n$ electron transitions.[6] This up-conversion process paves the way to initiate photodynamic (PDT) reaction with deeply penetrating NIR light and shall enable more efficient PDT at larger tissue volumes.

There are however two challenges to make this possible. Since the PDT may occur only upon efficient ET from UCNPs to photosensitiser, anchoring photosensitisers (PS) directly to UCNPs and finding PSs of appropriate excitation spectrum (i.e. overlapping the luminescence of up-converting lanthanides) is of critical importance.[7] In particular, ytterbium and erbium co-doped sodium yttrium fluoride ($NaYF_4$: $Er^{3+}$,$Yb^{3+}$) nanoparti[illegible] have been used as energy donors for different PSs, such a[illegible] $Ru(bpy)_3^{2+}$,[8] zinc phthalocyanine,[5, 9] merocyanine 540, hypericin,[11] methylene blue,[12,13] rose bengal,[3] pyropheophorbide a,[14] chlorin e6,[15] and a diiodo-bodip[illegible] compound.[16] These UCNPs have also proved successful energy donors to QDs[17] and other fluorescent dyes[18] such a[illegible] rhodamine 6G.[19] In all these systems, the spectral overlap o[illegible] the UCNP emission spectrum with the PS absorption spectr[illegible] is a pre-requisite for the efficient energy transfer (ET).

Moreover, for organic/inorganic fluorophores the ET yield (η) depends on the donor-to-acceptor separation distance ($r_{DA}$) with an inverse $6^{th}$ power law due to the dipole-dipol[illegible] coupling mechanism following simple relation $\eta=[1+(r_{DA}/R_0)^6]^{-1}$, where $R_0$ is Forster distance ($R_0$<10nm).[2]

For upconverting nanoparticles, there are numerous donor[illegible] within single nanoparticle, which display a whole range o[illegible] effective distances to acceptors anchored at the surface, and the photophysics behind UC-RET is a more comp[illegible]ex phenomenon.

Different strategies have been used to anchor the PS molecules as dense and as close to the surface as possible, b[illegible] grafting or adsorption to the surface, or by covalent linkage to the nanoparticle functional capping.

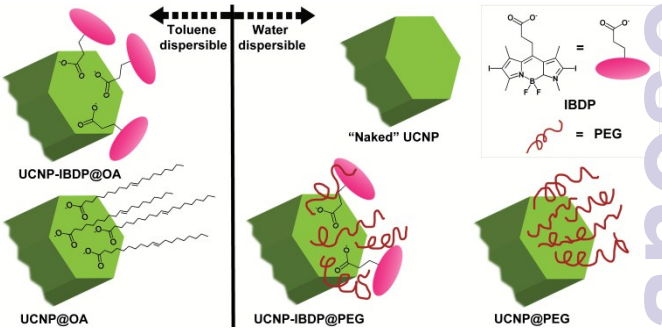


**Fig. 1.** Descriptive image illustrating the up-conversion nanoparticles with diffe[illegible] coatings and solubility selected for this study.

[a] *Instituto de Ciencia Molecular (ICMol)/Departamento de Química Orgánica, Universidad de Valencia, C/ Catedrático José Beltrán 2, 46980, Paterna, Valencia, Spain. Email: julia.perez@uv.es, maria.gonzalez@uv.es.*
[b] *IMDEA Energy Institute, Parque tecnológico de Móstoles, Avda. Ramón de la Sagra, 3, 28935, Móstoles, Madrid.*
[c] *Wrocław Research Centre EIT+, ul. Stabłowicka 147, 54-066 Wrocław, Poland.*
[d] *Department of Excited States Spectroscopy, Institute of Low Temperature and Structure Research, Polish Academy of Sciences, ul.Okolna 2, 50-422 Wroclaw, Poland.*

Electronic Supplementary Information (ESI) available: TEM pictures and their corresponding histograms, UV-Visible, power dependance plot and decay fittings. See DOI: 10.1039/c000000x/

In this context, we have recently designed a nanohybrid made of $NaYF_4$:$Yb^{3+}$, $Er^{3+}$ UCNPs and a diiodo-substituted Bodipy derivative (namely, 3-(2',6'-diiodo-1',3',5',7'-tetramethyl-4',4'-difluoro-4'-bora-3'a,4'a-diaza-s-indacen-8'yl) propanoic acid; IBDP), which is anchored to the nanoparticle surface directly and embedded in the organic capping (a polyethylenglycol, PEG, derivative).[16] This nanohybrid was dispersible in water due to its polymeric coating.

Now, to determine the efficiency of the energy transfer process between IBDP and the UCNP core in UCNP-IBDP nanohybrids, both steady-state and time-resolved emission measurements were carried out with water- or organic-dispersible nanohybrids (Figure 1). Nanohybrids were prepared from the same batch of oleate-capped UCNPs (UCNP@OA), and their photophysical properties were compared with those of the UCNP@OA and naked UCNPs ($UCNP_{naked}$), which also originated from the same UCNP@OA batch.

This made it possible to compare the influence of the nanoparticle capping and the solvent itself on the optical properties of the nanohybrids.

Upconversion nanoparticles ($NaYF_4$: $Yb^{3+}$ (16%), $Er^{3+}$ (4%)) capped with oleate (UCNP@OA) were synthesised following a protocol described in the literature with some modifications (see ESI Fig. S1-S3).[20] Transmission electron microscopy (TEM and high resolution TEM, HRTEM) showed that the UCNPs were uniform hexagonal prisms (38.4 ± 1.7 and 13.6 ± 1.4 nm, height and side, respectively, Fig. S1). Then, naked UCNPs ($UCNP_{naked}$) and UCNP@PEG[21] were synthesised by removing the oleate ligand of UCNP@OA by acidification with HCl[22], whereas UCNP@PEG were synthesised by exchange of the oleate with HS-PEG-$NH_2$[21] (See Fig. S4 and ESI for further details).

We have previously reported that the ligand exchange reaction of UCNP@PEG with IBDP led to water-dispersible nanohybrids (UCNP-IBDP@PEG)[16], see Fig. S5 and experimental details in ESI. Similar methods were applied to UCNP@OA nanoparticles in order to produce lipophilic hybrid (UCNP-IBDP@OA) nanoparticles. Briefly, a mixture of IBDP and the UCNP@OA was sonicated in water in the presence of triethylamine for 15 min to ensure the deprotonation of the IBDP carboxylic group and, consequently, its grafting to the UCNP surface.[22] Then, the mixture was stirred for 24 h in an orbital shaker at room temperature. Then, the nanoparticles were centrifuged and washed five times in acetonitrile in order to remove the excess of IBDP. Finally, the UCNP-IBDP@OA nanohybrid (pink powder) was re-suspended in toluene (See experimental details in the ESI).

The UV-Vis absorption spectra (Figure 2) and TGA analyses (not shown) of UCNP-IBDP@OA and UCNP-IBDP@PEG revealed an IBDP load of 40% and 10%, respectively. Figure 2 shows the comparison between the emission spectra of the water-dispersible nanoparticles, i.e., $UCNP_{naked}$, UCNP@PEG, and UCNP-IBDP@PEG on the left panel, while right panel compares the spectra of the toluene-dispersible nanoparticles, i.e., UCNP@OA and UCNP-IBDP@OA, after 975 nm excitation.

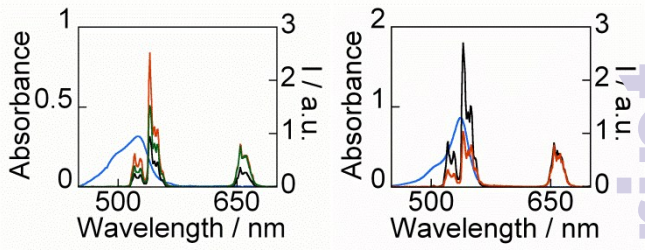


**Fig. 2.** (Left) UV-Visible absorption spectrum of IBDP in UCNP-IBDP@PEG (blue line); emission spectra of water solutions of UCNP naked (black line), UCNP@PEG (red line), and UCNP-IBDP@PEG (green line). (Right) UV-Visible absorption spectrum of IBDP in UCNP-IBDP@OA in toluene (blue line); emission spectra of toluene solutions of UCNP@OA (black line) and UCNP-IBDP@OA (red line). The spectra were recorded using a front face set-up after excitation at 975 nm. The green to red emission intensity ratio was found to be 3.2 (UCNP@OA), 1 (UCNP@IBDP), 2.5 (naked) and 2.5 (UCNP@PEG), and 1.8 (UCNP@IBDP@PEG) respectively. The UCNP-IBDP@PEG and UCNP-IBDP@OA solutions contained 1 mg of the nanohybrid and the IBDP concentration was 0.7 μM and 1.7 μM, respectively.

The UV-Visible absorption spectrum of IBDP has been included in both solvents to compare the overlap between the absorption spectrum of IBDP (the energy acceptor) and the emission of the UCNP (energy donor) in both water and toluene, as such overlap is a prerequisite for RET energy transfer to occur.[3, 5] The overlap is quantified with the spectral overlap integral ($J$) calculated as $J=\Sigma\, \sigma_D\,(\lambda)\sigma_D(\lambda)\lambda^4\delta\lambda$, where $\sigma_D$ is the normalized donor emission spectrum, the $\sigma_A$ is the acceptor molar extinction coefficient, and $\lambda$ is the wavelength of light.

Upon excitation at 975 nm (where $Yb^{3+}$ absorbs), the emission spectra of all the UCNPs exhibited three bands owing to Er emission: an intense band at 540 nm ($^4S_{3/2}\rightarrow{}^4I_{15/2}$), another close emission at 520 nm ($^2H_{11/2}$, $\rightarrow{}^4I_{15/2}$), and a red band at longer wavelengths (at ca. 670 nm, $^4F_{3/2}\rightarrow{}^4I_{15/2}$).[23] Power dependence measurements showed that emission was proportional to the 2nd power of excitation intensity, which is consistent with previously reported values (Figure S8).[24] As expected, all the bands of $UCNP_{naked}$ were less intense than those of the PEG-capped UCNP, which is consistent with the capacity of PEG to passivate the UCNP surface (Figure 1, left).

The comparison between the emission spectrum of each nanohybrid, UCNP-IBDP@PEG and UCNP-IBDP@OA, and its precursor, i.e., UCNP@PEG and UCNP@OA, respectively, revealed that the IBDP induced quenching of the green UCNP emission band, where IBDP absorption was present. The efficiency of the RET was calculated by using simple formula based on either emission intensity or emission lifetimes, $\eta = (I_D-I_{DA})/I_D = 1-\tau_{DA}/\tau_D$, where $I_{DA}$ and $I_D$ are the integrated emission of D-A nanohybrid (UCNP-IBDP@PEG and UCNP-IBDP@OA) and the respective nanohybrid precursor emission (UCNP@PEG and UCNP@OA), while $\tau_{DA}$ and $\tau_D$ are the luminescence lifetimes of D-A and D alone species, at the D emission wavelength. The intensities in the 513-560 nm range decreased by ca. 50% and 30% for UCNP-IBDP@OA and UCNP-IBDP@PEG, respectively (similar results were obtained when the intensities at 546 nm were compared). In quantitative terms, the $J$ overlap of UCNP-IBDP@OA in toluene was larger than that of UCNP-IBDP@PEG in water ($9.948\cdot10^{15}$ $nm^4$

$^{1}\cdot cm^{-1}$ and $1.226\cdot10^{13}$ $nm^{4}\cdot M^{-1}\cdot cm^{-1}$, respectively), but, as mentioned-above, the loading of IBDP was also larger in the former. No emission of energy acceptor molecules appeared in the nanohybrids, which is consistent with the negligible fluorescence quantum yield of IBDP ($\Phi_f$ = 0.02 in methanol).[25]

As a control experiment, small volumes of a toluene solution of a diiodobodipy lacking the carboxylic acid group (specifically, 4,4-difluoro-1,3,5,7,8-pentamethyl-4-bora-3a,4a-diaza-s-indacene), IBDPnc, $5\cdot10^{-3}$ M) were added to an oleate-capped UCNP dispersed in toluene (1 $mg\cdot ml^{-1}$) up to a final IBDPnc concentration of 0.45 mM. Figure S9 shows the decrease of the green emission with increasing concentrations of IBDPnc. It was expected that this substance would not anchor the UCNP surface and, consequently, the quenching of the UCNP emission was presumed to be due to filter effects.

To get insight into the nature of the intermolecular quenching process in the nanohybrids and corroborate the filter effects in the UCNP@OA/ IBDPnc mixtures, we carried out time-resolved measurements of all the UCNPs. The emission of UCNP@OA, recorded at 546 and 654 nm, showed no time-dependence in the presence of increasing IBDPnc concentrations up to the highest concentrations tested. This confirmed that the energy transfer in the intermolecular system occurred via a trivial emission-reabsorption mechanism.

The kinetic traces at $\lambda_{exc}$= 975 nm excitation for the $UCNP_{naked}$, UCNP@PEG, UCNP@OA, UCNP-IBDP@PEG, and UCNP-IBDP@OA showed characteristic rise and decay phases (Figure 3, Table 1, and ESI).[26] The rise and decay lifetimes ($\tau_{rise}$ and $\tau_{decay}$, respectively) were determined by fitting the data and these two components correspond to the sensitisation and subsequent decay of the $Er^{3+}$ excited state. All the fittings exhibited good quality match and the $\tau_{rise}$ and $\tau_{decay}$ decays were estimated by triplicate.

The decay lifetimes of the UCNP emission were in the tens to hundredths μs range and those for the red emission were longer (ca. 250-320 μs) than those of the green (65-125 μs), see Table 1. The fitted kinetics for each of the UCNPs is shown in the ESI (Fig S10-S20).

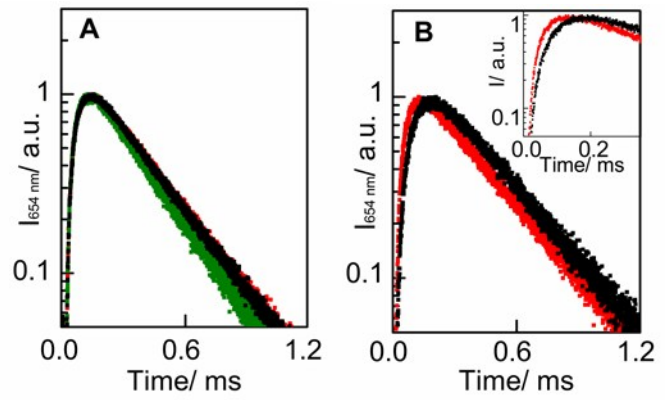


**Fig. 3.** Kinetic profiles at 654 nm of A) $UCNP_{naked}$ (black trace), UCNP@PEG (red trace), and UCNP-IBDP@PEG (green trace) in water and B) UCNP@OA (black trace) and UCNP-IBDP@OA (red trace) in toluene; amplification in the 0-0.2 ms time scale. Note that intensities are not real.

Table 1. Luminescence lifetimes for the UCNPs excited at 975 nm.[a]

| UCNP | $^4S_{3/2}\rightarrow{}^4I_{15/2}$[b] green emission | | $^4F_{9/2}\rightarrow{}^4I_{15/2}$[c] red emission | |
|---|---|---|---|---|
| | $\tau_{rise}$, μs | $\tau_{decay}$, μs | $\tau_{rise}$, μs | $\tau_{decay}$, μs |
| water dispersible | | | | |
| $UCNP_{naked}$ | 45±7 | 78±3 | 70±10 | 277±6 |
| UCNP@PEG | 44±5 | 82±2 | 69±7 | 281±4 |
| UCNP-IBDP@PEG | 54±7 | 67±2 | 63±7 | 252±4 |
| toluene dispersible | | | | |
| UCNP@OA | 94±4 | 119±1 | 122±18 | 304±8 |
| UCNP-IBDP@OA | 58±10 | 96±6 | 61±6 | 317±4 |

[a]Average value of three fittings. [b]$\lambda_{em}$=546 nm ,[c] $\lambda_{em}$= 654 nm.

In this study, we used the same batch of UCNP@OA for the preparation of the other four samples and no change in the crystalline phase, size, or shape of the UCNP core was detected upon hybrid formation.

Therefore, the observed differences in the decay lifetimes shall be attributed to non-radiative processes due to the interaction of the UCNPs with the solvent, the capping ligand, and, in the case of the nanohybrids, the diiodobodipy acceptor molecules. As expected, taking into account that O-H vibrations deactivate lanthanide excited states due to multiphonon non-radiative interactions,[27] the decay of the green and red emissions were longer for the UCNPs dispersed in toluene than in water (Table 1). This impact of the solvent was less pronounced for the red emission (*ca.* 300 vs 280 μs) as compared to green (*ca.* 80 vs 120 μs), which suggests that the population of higher energy levels and non-radiative deactivation of these levels are more susceptible to the presence of O-H vibrations.[2] Larger discrepancies can be observed for the luminescence risetimes, where the toluene dispersed UCNP@OA exhibited almost twice as long values (94 and 122 μs for green and red, respectively) as compared to water soluble UCNP@PEG (44 and 69 μs for green and red, respectively).

This observation demonstrates the fast saturation of intermediate excited state levels of $Er^{3+}$ ions in water dispersible UCNP@PEG NPs and most probably supports the hypothesis of critical role of $Yb^{3+}$ energy migration network in releasing the absorbed energy through the surface $Yb^{3+}$ ions.

In addition, the presence of IBDP in UCNP-IBDP@PEG led to a shortening of $\tau_{decay}$ (from 82 μs to 67 μs, $\eta=1-\tau_{DA}/\tau_D$ = 18%). A similar behaviour was observed for the green emission of the lipophilic nanohybrid ($\tau_{decay}$ of 119 μs and 96 μs, η=19%, for UCNP@OA and UCNP-IBDP@OA, respectively, Table 1).

The presence of IBDP in both UCNP-IBDP@PEG and UCNP-IBDP@OA demonstrated faster rise-times of red emission band kinetics, in comparison to non-IBDP NPs. This behavior indicates the IBDP plays a role in the up-conversion and changes the balance between ETU and depopulation phenomena during the intermediate steps despite the evident energy mismatch between the excited states of $Er^{3+}$ donors and energy levels of IBDP acceptor.

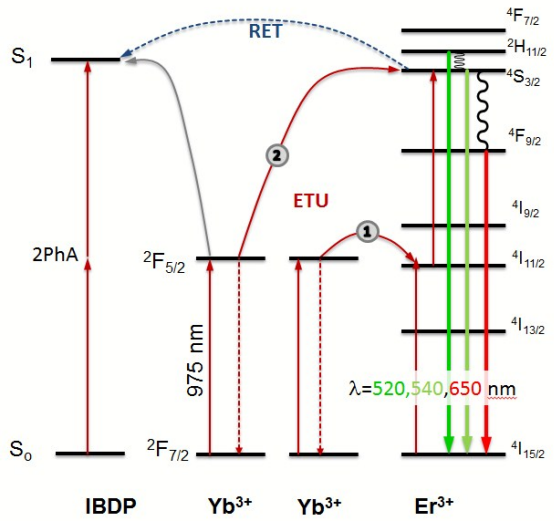


**Fig. 4.** Schematic picture showing the competitive energy transfer from $Yb^{3+}$ excited state ($Yb^{3+*}$) to $Er^{3+}$ and IBDP.

Moreover the red emission decays in UCNP-IBDP@PEG was *ca.* 10% shorter than that of UCNP@PEG, while UCNP-IBDP@OA exhibited the red decay to be slightly longer than the non IBDP nanohybrid. The interpretation of such relations is not straightforward and requires further investigations.

Regarding the risetimes ($\tau_{rise}$ of the green and red emission donor hybrids, again the hydrophilic UCNP@PEG NPs exhibited shorter lifetimes than UCNP@OA. Remarkably, the $\tau_{rise}$ of the UCNP-IBDP@OA green emission decreased almost two-fold as compared to that of UCNP@OA, and similar shortening was also detected for the $\tau_{rise}$ of the red emission. Such consistent behaviour was not observed for PEG coated NPs.

A likely interpretation for the lipophilic UCNP-IBDP@OA could be that the presence of IBDP makes a competitive decay possible for the metastable state of $Yb^{3+}$ ($Yb^{3+*}$). Specifically, $Yb^{3+*}$ could be involved in the population not only of $Er^{3+}$ excited states but also in that of IBDP (IBDP*) after absorption of a second photon (Figure 4). As a consequence, the risetime of both red and green emissions would reflect the decrease of the contribution of $Yb^{3+*}$ to populate the $Er^{3+}$ excited states involved in those emissions.

To corroborate this hypothesis we prepared the lipophilic $Yb^{3+}(IBDP)_3$ complex (see ESI for experimental details) which was excited at 975 nm. Remarkably, the anti-Stokes IBDP fluorescence (Figure 5 left, in blue) was detected in spite of the considerably low absorption cross section of the $Yb^{3+}$ ions (as compared to Stokes excitation of IBDP) at the NIR and the low fluorescence of the diiodo-Bodipy.

This suggested that the $Yb^{3+}(IBDP)_3$ complex can up-convert following the proposed scheme

$$Yb^{3+}\text{-IBDP} + h\nu_1 \rightarrow Yb^{3+*}\text{-IBDP}$$
$$Yb^{3+*}\text{-IBDP} + h\nu_1 \rightarrow Yb^{3+}\text{-IBDP*}$$
$$Yb^{3+}\text{-IBDP*} \rightarrow Yb^{3+}\text{-IBDP} + h\nu_2 \ (h\nu_2 > h\nu_1)$$

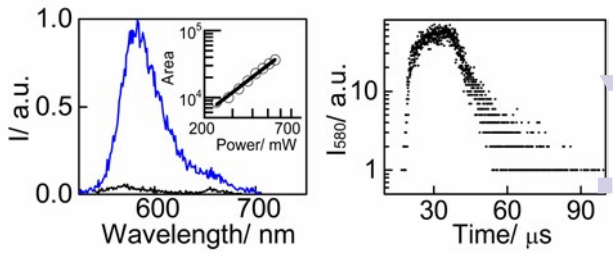


**Fig. 5.** Left: comparison between the emission spectra of IBDP (black) and of $Yb^{3+}(IBDP)_3$ complex in toluene under NIR 975 nm excitation. The inset demonstrates the power dependence - the anti-Stokes emission intensity, which is proportional to the 2nd power of excitation intensity. Right: kinetic time profile of the anti-Stokes IBDP emission in $Yb^{3+}(IBDP)_3$ under 975 nm laser excitation.

It is known that Bodipy compounds are capable to undergo two-photon absorption processes.[28] Therefore, control experiments were carried out to confirm the involvement of the lanthanide in the emission of IBDP in the $Yb^{3+}(IBDP)_3$ when being excited at 975 nm. Figure 5 left shows the much more efficient emission of the Bodipy in the complex. Moreover, time-resolved measurements evidenced that the emission lifetime of $Yb^{3+}$-IBDP* was ca. 5 μs (Figure 5 right), a great deal longer than that of IBDP*, whose emission lifetime was but a few ns. Finally, power-dependence measurements corroborated that the IBDP emission after NIR excitation of $Yb^{3+}(IBDP)_3$ was proportional to the 2nd power of the 975 nm excitation intensity (inset Figure 5 right). The latter observation evidenced the need to involve two low energy 975 nm photons, to get visible emission of IBDP.

## Conclusions

We have prepared hydrophobic and hydrophilic UCNP-IBDP nanohybrids, which showed a decrease in their green to red emission compared to that of their precursors. Time-resolved experiments demonstrated that the quenching of the green emission was due to energy transfer from the UCNP to the anchored IBDP. Furthermore, the decrease in the efficiency of green and red emissions in UCNP-IBDP was attributed to the competitive decay of $Yb^{3+*}$ via energy transfer to IBDP after absorption of a second photon. This process was more competitive in the organic solvent. Therefore, the comparison between the emission risetimes, as well as between the emission decay lifetimes, of the nanohybrids and those of $UCNP_{naked}$, UCNP@PEG, and UCNP@OA, give valuable information about the excited states involved in UCNP emission kinetics.

## Acknowledgements

We thank the Spanish Ministry of Economy and Competitiveness (Projects CTQ2014-60174; M.G.B. Ramón y Cajal contract and L.F.S. F.P.U. grant). The work was partially supported by the grant DEC-2012/05/E/ST5/03901 from Narodowe Centrum Nauki, Poland.

## Notes and references


1. A. R. Clapp, I. L. Medintz, H. T. Uyeda, B. R. Fisher, E. R. Goldman, M. G. Bawendi and H. Mattoussi, *J. Am. Chem. Soc.*, 2005, **127**, 18212-18221.
2. T. Riuttamäki, I. Hyppänen, J. Kankare and T. Soukka, *J. Phys. Chem. C*, 2011, **115**, 17736-17742.
3. K. Liu, X. Liu, Q. Zeng, Y. Zhang, L. Tu, T. Liu, X. Kong, Y. Wang, F. Cao, S. A. G. Lambrechts, M. C. G. Aalders and H. Zhang, *ACS Nano*, 2012, **6**, 4054-4062.
4. Y. Wang, K. Liu, X. Liu, K. Dohnalová, T. Gregorkiewicz, X. Kong, M. C. G. Aalders, W. J. Buma and H. Zhang, *J. Phys. Chem. Lett.*, 2011, **2**, 2083-2088.
5. M. Wang, Z. Chen, W. Zheng, H. Zhu, S. Lu, E. Ma, D. Tu, S. Zhou, M. Huang and X. Chen, *Nanoscale*, 2014, **6**, 8274-8282.
6. A. Gnach and A. Bednarkiewicz, *Nano Today*, 2012, **7**, 532-563; F. Wang, D. Banerjee, Y. Liu and X. C. X. Liu, *Analyst*, 2010, **135**, 1839–1854.
7. C. Wang, L. Cheng and Z. Liu, *Theranostics*, 2013, **3**, 317-330.
8. Y. Guo, M. Kumar and P. Zhang, *Chem. Mater.*, 2007, **19**, 6071–6072.
9. H. Guo, H. Qian, N. M. Idris and Y. Zhang, *Nanomedicine*, 2010, **6**, 486–495; H. S. Qian, H. C. Guo, P. C.-L. Ho, R. Mahendran and Y. Zhang, *Small*, 2009, **5**, 2285–2290; S. Cui, H. Chen, H. Zhu, J. Tian, X. Chi, Z. Qian, S. Achilefuc and Y. Gu, *J. Mater. Chem.*, 2012, **22**, 4861-4873; S. Cui, D. Yin, Y. Chen, Y. Di, H. Chen, Y. Ma, S. Achilefu and Y. Gu, *ACS Nano*, 2013, **7**, 676-688; Q. Xiao, Y. Ji, Z. Xiao, Y. Zhang, H. Lin and Q. Wang, *Chem. Commun.*, 2013, **49**, 1527-1529.
10. P. Zhang, W. Steelant, M. Kumar and M. Scholfield, *J. Am. Chem. Soc.*, 2007, **129**, 4526-4527.
11. X. Yang, Q. Xiao, C. Niu, N. Jin, J. Ouyang, X. Xiao and D. He, *J. Mater. Chem. B*, 2013, **1**, 2757–2763.
12. F. Chen, S. Zhang, W. Bu, Y. Chen, Q. Xiao, J. Liu, H. Xing, L. Zhou, W. Peng and J. Shi, *Chem. Eur. J.*, 2012, **18**, 7082-7090.
13. L. Francés-Soriano, M. González-Béjar and J. Pérez-Prieto, *Nanoscale*, 2015, **7**, 5140-5146.
14. A. Zhou, Y. Wei, B. Wu, Q. Chen and D. Xing, *Mol. Pharmaceutics*, 2012, **9**, 1580-1589.
15. C. Wang, L. Cheng and Z. Liu, *Biomaterials*, 2011, **32**, 6145-6154; Y. I. Park, H. M. Kim, J. H. Kim, K. C. Moon, B. Yoo, K. T. Lee, N. Lee, Y. Choi, W. Park, D. Ling, K. Na, W. K. Moon, S. H. Choi, H. S. Park, S.-Y. Yoon, Y. D. Suh, S. H. Lee and T. Hyeon, *Adv. Mater.*, 2012, **24**, 5755-5761.
16. M. González-Béjar, M. Liras, L. Francés-Soriano, V. Voliani, V. Herranz-Pérez, M. Duran-Moreno, J. M. Garcia-Verdugo, E. I. Alarcon, J. C. Scaiano and J. Pérez-Prieto, *J. Mater. Chem. B*, 2014, **2**, 4554-4563.
17. L. Mattsson, K. D. Wegner, N. Hildebrandt and T. Soukka, *RSC Advances*, 2015, **5**, 13270-13277; A. Bednarkiewicz, M. Nyk, M. Samoc and W. Strek, *J. Phys. Chem. C*, 2010, **114**, 17535-17541 ; C. Yan, A. Dadvand, F. Rosei and D. F. Perepichka, *J. Am. Chem. Soc.*, 2010, **132**, 8868-8869; Z. Li, Y. Zhang and S. Jiang, *Adv. Mater.*, 2008, **20**, 4765-4769; T. L. Nguyen, P. Spizzirri, G. Wilson and P. Mulvaney, *Chem. Commun.*, 2009, 174-176.
18. X. Li, F. Zhang and D. Zhao, *Chem. Soc. Rev.*, 2015, **44**, 1346-1378.
19. R. Chen, V. D. Ta, F. Xiao, Q. Zhang and H. Sun, *Small*, 20[illegible] **7**, 1052-1057.
20. Z. Li and Y. Zhang, *Nanotechnology*, 2008, **19**, 345606.
21. V. Voliani, M. González-Béjar, V. Herranz-Pérez, M. Duran Moreno, G. Signore, J. M. Garcia-Verdugo and J. Pérez-Prieto, *Chem. Eur. J.*, 2013, **19**, 13538-13546.
22. N. Bogdan, F. Vetrone, G. A. Ozin and J. A. Capobianco, *Nano Lett.*, 2011, **11**, 835-840.
23. J.-C. Boyer, F. Vetrone, L. A. Cuccia and J. A. Capobianco, *J. Am. Chem. Soc.*, 2006, **128**, 7444-7445; F. Auzel, *Chem. Rev.*, 2004, **104**, 139–173
24. V. F. Boyer J-C, Cuccia L A, Capobianco J A, *J. Am. Chem. Soc.*, 2006, **128**, 7444-7445.
25. T. Yogo, Y. Urano, Y. Ishitsuka, F. Maniwa and T. Nagano, *J. Am. Chem. Soc.*, 2005, **127**, 12162-12163.
26. M. P. Hehlen, G. Frei and H. U. Güdel, *Phys. Rev. B*, 1994, **50**, 16264-16273.
27. Q. Lü, F. Guo, L. Sun and A. Li, *J. Phys. Chem. C*, 2008, **112**, 2836-2844.
28. X. Zhang, Y. Xiao, J. Qi, J. Qu, B. Kim, X. Yue and K. D. Belfield, *J. Org. Chem.*, 2013, **78**, 9153-9160.